# Dielectric Relaxation and Rheological Behavior of Supramolecular Polymeric Liquid

**8 AUTHORS**, INCLUDING:

Nan Lou
Shanghai Jiao Tong University
**2** PUBLICATIONS   **20** CITATIONS

SEE PROFILE

Xiaopeng Li
University of Akron
**44** PUBLICATIONS   **1,043** CITATIONS

SEE PROFILE

Chrys Wesdemiotis
University of Akron
**259** PUBLICATIONS   **5,721** CITATIONS

SEE PROFILE

Huiming Xiong
Shanghai Jiao Tong University
**44** PUBLICATIONS   **814** CITATIONS

SEE PROFILE

# Dielectric Relaxation and Rheological Behavior of Supramolecular Polymeric Liquid

Nan Lou,[†] Yangyang Wang,[‡] Xiaopeng Li,[§,‖] Haixia Li,[†] Ping Wang,[⊥] Chrys Wesdemiotis,[§] Alexei P. Sokolov,[‡] and Huiming Xiong*,[†]

[†]Department of Polymer Science, Shanghai Jiao Tong University, Shanghai 200240, P. R. China
[‡]Chemical Sciences Division, Oak Ridge National Laboratory, Oak Ridge, Tennessee 37831, United States
[§]Department of Chemistry and Polymer Science, University of Akron, Akron, Ohio 44325, United States
[‖]Department of Chemistry and Biochemistry, Texas State University, San Marcos, Texas 78666, United States
[⊥]Dow Chemicals Company Limited, Shanghai 201203, P. R. China

Ⓢ Supporting Information

**ABSTRACT:** A model self-complementary supramolecular polymer based on thymine and diamidopyridine triple hydrogen-bonding motifs has been synthesized, and its dielectric and rheological behavior has been investigated. The formation of supramolecular polymers has been unequivocally demonstrated by nuclear magnetic resonance, electrospray ionization mass spectrometry with traveling wave ion mobility separation, dielectric spectroscopy, and rheology. The dynamical behaviors of this associating polymer generally conform to those of type-A polymers, with a low-frequency chain relaxation and a high-frequency $\alpha$ relaxation visible in both rheological and dielectric measurements. The dielectric chain relaxation shows the ideal symmetric Debye-like shape, resembling the peculiar features of hydrogen-bonding monoalcohols. Detailed analysis shows that there exists a weak decoupling between the mechanical terminal relaxation and dielectric Debye-like relaxation. The origin of the Debye-like dielectric relaxation is further discussed in the light of monoalcohols.
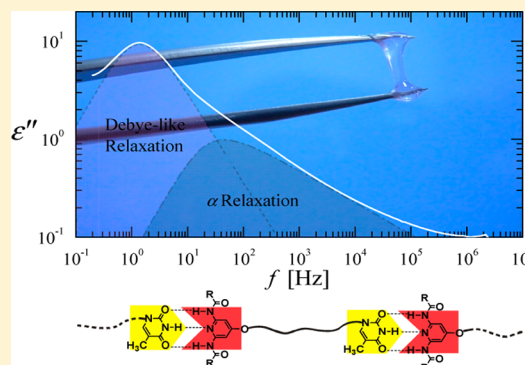
## INTRODUCTION

Supramolecular polymers have continuously attracted considerable attention due to their fundamental and technological importance. In contrast to conventional polymers made of covalently bonded backbones, supramolecular polymers are formed by linking monomers with reversible and relatively weak noncovalent interactions such as hydrogen bonding, metal coordination, and $\pi-\pi$ interaction.[1−13] The reversible nature of these noncovalent bonds brings about extra complexity, making the understanding of local and global dynamics a challenge. While a lot of effort has been devoted to constructing supramolecular polymers through diverse structural building blocks, much less attention has been paid to the dynamics of this important class of material. For example, the dielectric behavior of supramolecular polymers has rarely been reported.[14,15] On the theoretical side, numerous models have proposed to describe the dynamical behavior of supramolecular or "living" polymers[16−22] and associating polymers[23−31] in general. However, direct comparison between theory and experiment, especially for supramolecular polymer in unentangled state, is still quite limited.[17,22,27]

In this article, we report the dielectric and rheological behavior of a model self-complementary supramolecular polymer which is based on the triple hydrogen-bonding thymine and diamidopyridine motifs.[32] In contrast to the widely studied ureidopyrimidone-based (UPy) materials,[33] the strength of hydrogen-bonding interaction of T-DAP9 is in the medium range, bridging between that of UPy and hydrogen bonds of single valence. Besides, this supramolecular polymer appears completely amorphous in the molten state with a thermal glass transition temperature around 0 °C and thus may serve as a model system for the study of dynamics of this class of associating liquid. The formation of supramolecular polymer is confirmed by solution nuclear magnetic resonance, electrospray ionization mass spectrometry with traveling wave ion mobility separation, dielectric spectroscopy, and rheology. The dielectric spectrum of the supramolecular polymer typically consists of a prominent Debye-like relaxation and a weak high-frequency relaxation, similar to what has been observed in hydrogen-bonding liquids such as monoalcohols, whose exact nature has remained a "puzzle" for one century.[34] The Debye-like process is found to be closely related to zero-shear viscosity, whereas the high-frequency process is identified as the structural relaxation. The general rheological and dielectric
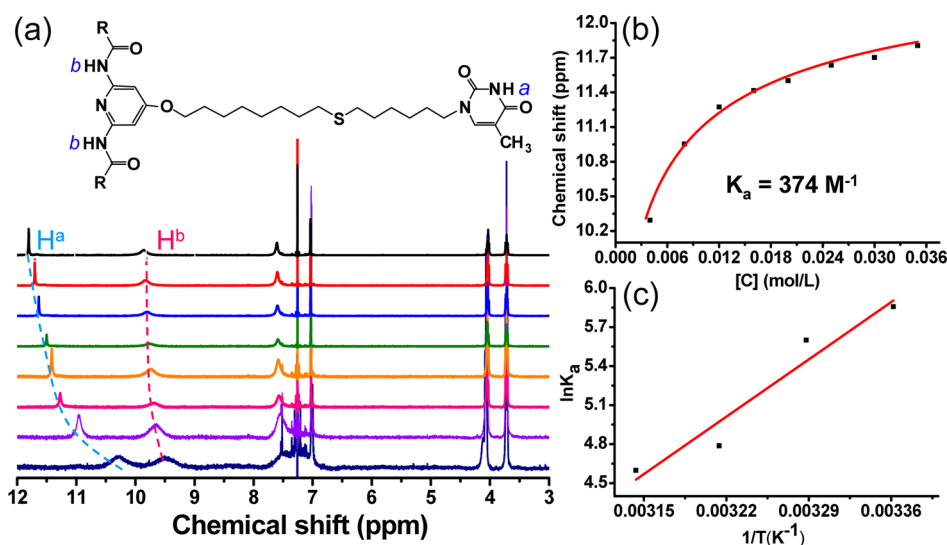
**Figure 1.** (a) $^1$H NMR spectra of T-DAP9 in CDCl$_3$ at 297 K in different concentrations (from bottom to top: 4, 8, 12, 16, 20, 25, 30, and 35 mM). The chemical structure of T-DAP9 is shown at the top. Here, R: $-(CH_2)_8CH_3$. (b) Determination of the association constant of T-DAP9 in CDCl$_3$ at 297 K. Fitting is based on chemical shifts of H$^a$. (c) Temperature dependence of associate constants of T-DAP9. Solid curve: fitting according to the van't Hoff equation.

behavior of the supramolecular polymer resembles type-A polymers with a very weak decoupling between the mechanical terminal relaxation time and dielectric Debye-like relaxation. The physical origin of the dielectric Debye-like relaxation is further discussed.

## ■ EXPERIMENTAL SECTION

**1. Materials.** The self-complementary triple hydrogen-bonding AB-type molecule, referred to as T-DAP9, is based on thymine (T) and diamidopyridine (DAP) motifs. The two hydrogen-bonding parts (T and DAP) are covalently connected by the thiol−ene "click" chemistry. In addition, two long alky chains $[-(CH_2)_8CH_3]$ have been attached to the DAP end, which results in a substantial decrease of thermal glass transition temperature ($T_g$ = 266 K) of the target molecule in comparison to T-DAP molecules.[32] The details of synthesis and characterization by $^1$H NMR are described in the Supporting Information and can be also referred to ref 32. Compared to the commonly used ureidopyrimidone motif, the strength of hydrogen-bonding in T-DAP9 is much weaker. Therefore, supramolecular polymers of relatively low molecular weight should be expected.

**2. Characterization.** *2.1. Nuclear Magnetic Resonance (NMR) Spectroscopy.* T-DAP9 solutions of different concentrations (0.004, 0.008, 0.012, 0.016, 0.020, 0.025, 0.030, and 0.035 mol/L) in deuterated chloroform CDCl$_3$ were prepared for NMR measurements. Temperature dependence of NMR spectra of these solutions was carried out at four different temperatures (297, 304, 311, and 318 K).

*2.2. Electrospray Ionization Mass Spectrometry (ESI-MS) and Electrospray Ionization−Traveling Wave Ion Mobility Mass Spectrometry (ESI-TWIM MS).* Both ESI MS and ESI-TWIM MS experiments were performed with a Synapt HDMS quadrupole/time-of-flight mass spectrometer (Waters Corporation) to detect the exact masses of the associating polymers formed by T-DAP9. The sprayed solutions were prepared by dissolving 0.1 mg of sample in 1 mL of methanol/CH$_2$Cl$_2$ (v/v, 30/70) or methanol/tetrahydrofuran (v/v, 30/70). A few droplets of a 10 mg/mL sodium trifluoroacetate (NaTFA) solution in the same solvent were added to the sprayed mixture. Tandem MS experiments combined with TWIM separation were performed in a trap cell (fragmentation before ion mobility separation). All tandem MS studies employed 4−110 eV collisions with argon targets. Data analysis was conducted with the MassLynx 4.1 and DriftScope 2.1 programs from Waters.

*2.3. Dielectric Spectroscopy.* Dielectric measurements were conducted in the frequency range of $10^{-1}$−$10^7$ Hz on a Novocontrol Concept 80 system with Alpha-A impedance analyzer and Quatro Cryosystem temperature control. The sample melt was carefully vacuumed and placed between two round plate gold electrodes, with a Teflon ring in thickness of 54 $\mu$m as a spacer. The dielectric measurements started from 393 K and ended at 297 K, above the thermal glass transition temperature.

*2.4. Rheology.* Rheological measurements of T-DAP9 were carried out on an AR2000ex rheometer from TA Instruments. Temperature control was achieved by using an environmental testing chamber with nitrogen as the gas source. The experiments started from cooling at 348 K and ended at 297 K. Both creep and small-amplitude oscillatory shear measurements were performed to determine the linear viscoelastic properties of the sample. The zero-shear viscosity was evaluated from the creep measurements as $\eta_0 = \lim_{t\to\infty}(t/J(t))$, where $J(t)$ is the transient shear compliance.

## ■ RESULTS

**1. NMR Spectroscopy.** Solution NMR spectroscopy is one of the most common experimental techniques for characterizing the formation of associating polymers. Association through hydrogen bonding will affect the chemical shifts of the corresponding protons. Figure 1a shows that the chemical shifts of the hydrogen H$^a$ in thymine and H$^b$ in diamidopyridine go to the downfield with increasing concentration of T-DAP9 in CDCl$_3$. This implies that the degree of association becomes higher in concentrated solutions. In general, the chemical shifts of H$^a$ and H$^b$ depend on not only the T-DAP9 concentration but also the temperature. The equilibrium constant, change of enthalpy and entropy related to breakage and recombination of hydrogen bonding, and the average chain length can be calculated based on the solution NMR experiments, using the scission-recombination model[18−20,22] and van't Hoff equation. The details of these calculations are presented in the Discussion section.

**2. Mass Spectrometry.** By applying electrospray ionization (ESI) mass spectrometry coupled with traveling wave ion mobility (TWIM) separation, we were able to directly obtain the exact masses of the supramolecular species based on the molecular mass of T-DAP9 ($m$ = 785.6).[35−39] As shown in

Figure 2a, charge states are superimposed in conventional ESI-MS due to the low mass resolution under mild separation
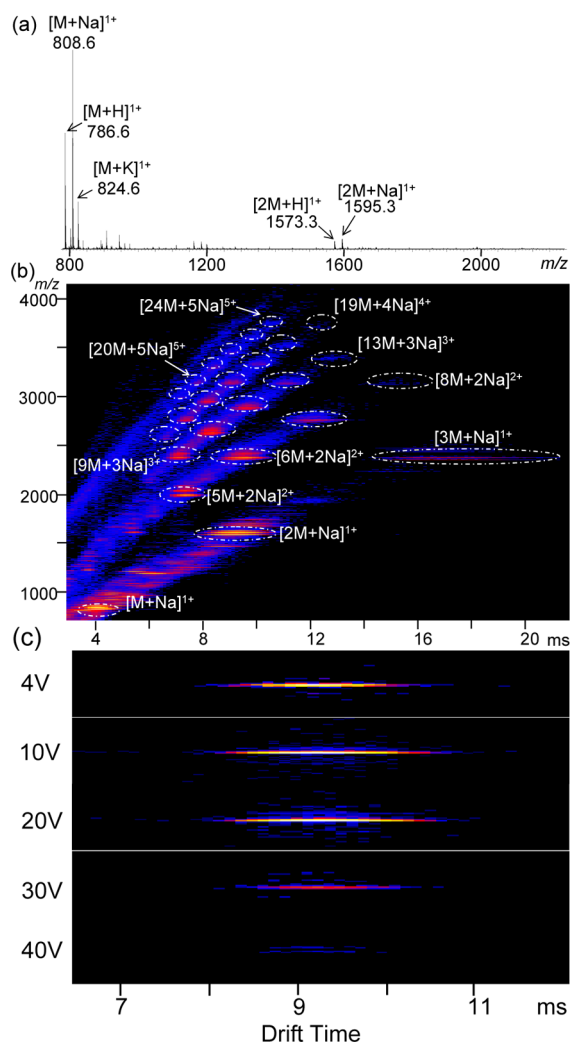


**Figure 2.** (a) Conventional ESI and (b) two-dimensional ESI-TWIM mass spectra of T-DAP9. (c) Two-dimensional gMS² TWIM plot of [2M + Na]$^{1+}$ at $m/z$ = 1595.3. Collisionally activated dissociation took place in the trap cell (before ion mobility separation) at different energies, which was varied by raising the potential applied to the trap from 4 to 40 V. The ions exiting the trap were subsequently separated in the ion mobility region.

conditions. With the aid of TWIM separation, five different charge states, i.e., 1+ to 5+, can be distinguished in the ESI-TWIM mass spectra, as shown in Figure 2. Monomer, dimer, trimer, and tetramer as well as other high-molecular-weight species can be observed. The largest identified species contains 24 repeating units.

Furthermore, gradient tandem mass spectrometry (gMS²) interfaced with ion mobility separation[38] was used to address the question of whether the high-molecular-weight species are assemblies due to hydrogen bonding or aggregates from weak van der Waals interaction. [2M + Na]$^{1+}$ dimer was selected in collisionally activated dissociation measurements. As shown in Figure 2C, its signal remains unchanged at 4, 10, and 20 V, starts to decrease at 30 V, and almost disappears at 40 V, which corresponds to a center-of-mass collision energy of 0.98 eV (95 kJ/mol). This experiment provides direct evidence that the formation of dimers is a result of strong hydrogen-bonding

interaction. Otherwise, the dissociation of dimers should have been observed at much lower voltage.

**3. Dielectric Spectroscopy.** Figure 3 presents the dielectric spectra of T-DAP9 at various temperatures. Two
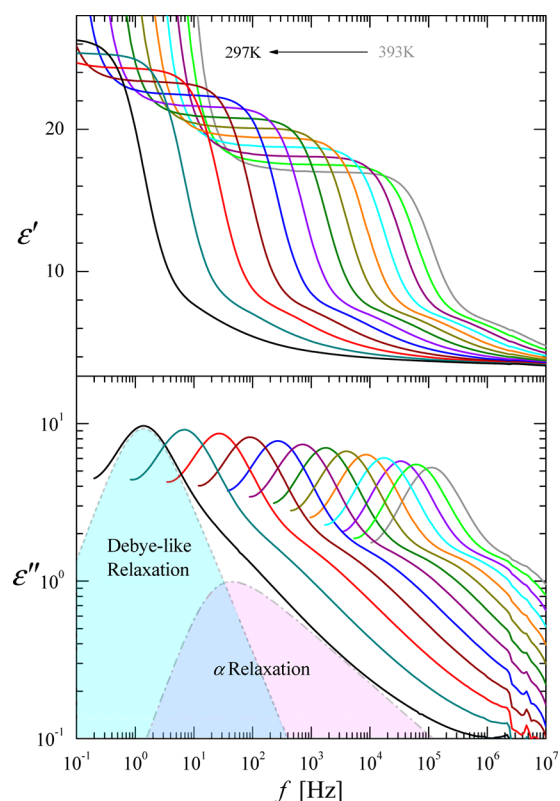


**Figure 3.** Representative dielectric spectra of T-DAP9 at various temperatures, where the real (the top) and imaginary (the bottom) parts of permittivity are plotted as a function of frequency. The temperature step is 4 K cooling from 393 to 297 K. For the sake of clarity, the response due to dc conduction has been truncated.

relaxation processes can be clearly seen from both the real and imaginary parts of the complex dielectric permittivity $\varepsilon^*$. The low-frequency relaxation has a Debye-like shape, whereas the high-frequency relaxation is stretched. The complex dielectric permittivity can be effectively described by the superposition of a Debye function, a Havriliak–Negami function,[40] and a dc conductivity term, as also demonstrated in Figure S5 of the Supporting Information:

$$\varepsilon^*(\omega) = \varepsilon_\infty + \frac{\Delta\varepsilon_1}{1 + i\omega\tau_1} + \frac{\Delta\varepsilon_2}{[1 + (i\omega\tau_2)^\alpha]^\beta} + \frac{\sigma}{i\varepsilon_0\omega} \quad (1)$$

The parameter $\varepsilon_\infty$ is the high-frequency limiting dielectric permittivity, $\Delta\varepsilon_i$ is the relaxation strength, $\tau_i$ is the relaxation time, $\alpha$ and $\beta$ are the shape parameters, and $\sigma$ is the dc conductivity. The dielectric spectra have been shifted with respect to the peak position of the Debye-like relaxation, as shown in Figure S6, where the Debye-like mode does not show any dispersion at various temperatures.

We label the high-frequency relaxation as the $\alpha$ relaxation (see the Discussion section), which is stretched in the high-frequency side, with $\alpha$ close to 1 and $\beta$ in the range 0.3–0.4. The relaxation strengths of the Debye-like relaxation and $\alpha$ relaxation are shown as a function of reciprocal temperature in Figure 4a. The strength of the Debye-like relaxation is more
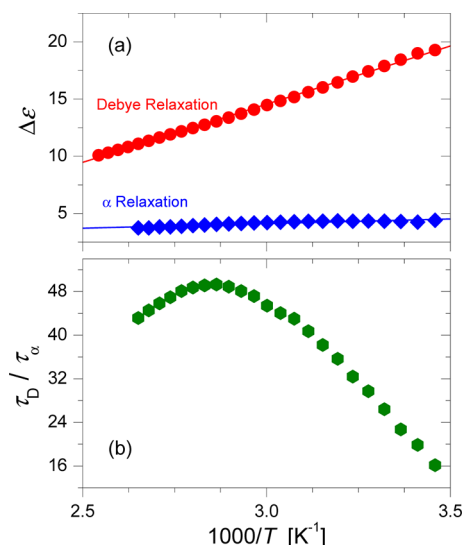
**Figure 4.** (a) Temperature dependence of the relaxation strength $\Delta\varepsilon$ of the Debye-like relaxation and $\alpha$ relaxation. (b) Temperature dependence of the ratio of the Debye-like relaxation time ($\tau_D$) and $\alpha$ relaxation time ($\tau_\alpha$).

sensitive to the temperature, and its strength increases about 2 times when the temperature is varied from 393 to 289 K. In comparison, the $\alpha$ relaxation strength does not show significant change in the same temperature range.

Figure 4b presents how the ratio of the relaxation times of the two processes varies with temperature. The temperature dependence of each process can be referred to the Discussion section. In the low-temperature region, $\tau_D/\tau_\alpha$ decreases with decrease of temperature. This trend is similar to what has been observed for the chain and segmental relaxation of other polymers, where the reduction in separation of the two relaxation processes is related to the decoupling phenomenon.[41,42] The opposite temperature dependence is observed in the high-temperature region and might be explained by the domination of the average chain length change with temperature.

**4. Rheology.** The results of small-amplitude oscillatory shear measurements are presented in Figure 5, in both modulus and compliance representation. The spectra at different temperatures have been horizontally shifted using the shift factor $a_T$ defined by viscosity: $a_T = \eta(T)/\eta(T_{ref})$. Here, the viscosities are from creep measurements, as illustrated in Figure S7; the reference temperature $T_{ref}$ is 20 °C. This construction, by definition, collapses the imaginary parts of $G^*$ and $J^*$ at low frequency. However, the real parts at different temperatures cannot be superimposed, indicating a breakdown of the time–temperature superposition principle.[43]

Two relaxation processes are clearly observed in the linear viscoelastic spectra, as shown in Figure 5 (a). The spectrum in the low-frequency region exhibits the terminal flow behavior, where $G' \sim \omega^2$ and $G'' \sim \omega$. The change of frequency dependence of $G'$ and $G''$ above 1 MPa is clearly recognizable, suggesting the emergence of polymeric chain modes. Above ~10 MPa, the glassy modes start to interfere. The high-frequency process is associated with the structural relaxation,[44] whereas the low-frequency process can be related to the relaxation of living chains. The emergence of a separate chain relaxation mode is also consistent with the observation of supramolecular polymers by our other experimental techniques.
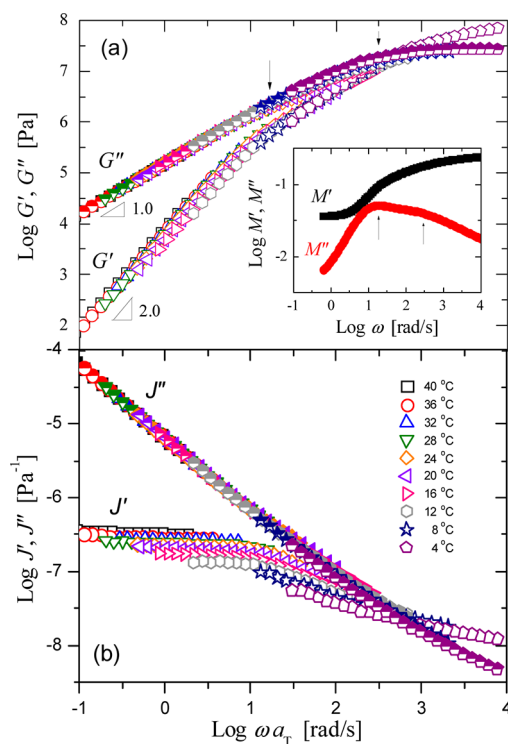


**Figure 5.** Linear viscoelastic spectra of the T-DAP9 molecule: (a) dynamic modulus $G'$ and $G''$ as a function of frequency $\omega a_T$; (b) dynamic compliance $J'$ and $J''$ as a function of frequency $\omega a_T$. Here, $a_T$ is the shift factor with respect to 20 °C: $a_T = \eta(T)/\eta(20$ °C$)$. Inset of (a): frequency dependence of electrical modulus $M'$ and $M''$ at 20 °C.

In addition, the spectrum shape of T-DAP9 is substantially different from small molecules and resembles that of low-molecular-weight polymers.[43,45]

The corresponding dielectric spectra at the reference temperature are shown in the inset of Figure 5a, in modulus ($M$) presentation. It becomes apparent that the dielectric $\alpha$ relaxation indeed corresponds to the mechanical structural relaxation, whereas the dielectric Debye-like relaxation is closely related to the mechanical terminal relaxation. A detailed discussion about these two dielectric relaxation processes as well as their relation to stress relaxation is presented in the following section.

## ■ DISCUSSION

**1. Average Chain Length.** An important issue in study of supramolecular polymers is the estimation of its chain length. For T-DAP9, while the ESI-TWIM MS experiments can provide a direct identification of associating chains up to 24 repeating units, it is not straightforward to calculate the average chain length $\bar{N}$ from such measurements. Nonetheless, $\bar{N}$ can be estimated based on solution NMR experiment and rheological measurement as well.

By measuring the chemical shifts in NMR spectra at various concentrations, the association constant $K_a$ can be obtained, as described in the Supporting Information. An example is given in Figure 1b. The association constant is estimated to be 374 $M^{-1}$ at 297 K, which is found to be 2 orders of magnitude higher than that of thymine[46] and diamidopyridine derivatives[47] but still substantially smaller than that of ureidopyrimidone.[33]

The average chain length $\bar{N}$ can be estimated by using the well-known Carothers equation, which relates $\bar{N}$ to the extent of conversion $p$[48]

$$\bar{N} = 1/(1 - p) = 2K_a[H]_0/\{(1 + 4K_a[H]_0)^{1/2} - 1\} \tag{2}$$

where $[H]_0$ is the concentration of the monomer. In the case of $(2K_a[H]_0)^{1/2} \gg 1$, $\bar{N} \approx (2K_a[H]_0)^{1/2}$. In the limit of bulk state, $[H]_0 = \rho/M_0$, where $\rho$ is the density of the sample and $M_0$ is the molecular weight of the T-DAP9 monomer. This calculation yields $\bar{N} \sim 26$ at 297 K. However, one should bear in mind that the physical environment in the bulk state can be different; therefore, the $K_a$ of the melt can vary from that in solution and thus $\bar{N}$.

The enthalpy and entropy change ($\Delta H$ and $\Delta S$) associated with hydrogen bonding can be derived using the association constants obtained by NMR experiments at different temperatures, based on the van't Hoff equation:

$$\ln K_a = -\frac{\Delta H}{RT} + \frac{\Delta S}{R} \tag{3}$$

where $R$ is the gas constant. The determination of $\Delta H$ and $\Delta S$ is shown in Figure 1c. The calculated enthalpy change $\Delta H$ is $-52$ kJ/mol, and the entropy change $\Delta S$ is $-127$ J/(K mol). With these values, we can obtain the association constant $K_a$ at a given temperatures. For example, $K_a \sim 33$ M$^{-1}$ at 333 K, which leads to $\bar{N} \sim 8$ based on eq 2. The moderate value of $\Delta H$ appears to be reasonable for the medium strength of the triple hydrogen bonds in T-DAP9. On the other hand, the $\Delta S$ of association of T-DAP9 is comparable with the entropy change in polymerization of other monomers, which is typically on the order of $-100$ J/(K mol).[49]

It is also possible to estimate the average chain length from the mechanical measurements. Figure 6 shows the steady-state
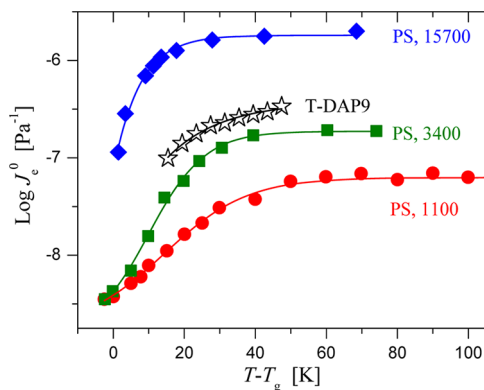


**Figure 6.** Steady-state creep compliance as a function of $T - T_g$. The polystyrene (PS) data are reproduced from ref 50. The lines are guides for the eyes.

creep compliance $J_e^0$ of T-DAP9 and several polystyrenes (PS)[50] as a function of $T - T_g$. Here, $J_e^0$ of T-DAP9 is determined from the value of $J'$ in the low-frequency limit. It is worth noting that $J_e^0$ of molecular liquids is typically on the order of $10^{-8}$–$10^{-9}$ Pa$^{-1}$. The $J_e^0$ of oligomers usually increases linearly with the molecular weight until the onset of chain entanglement.[51] The $J_e^0$ of T-DAP9 is $\sim 10^{-7}$ Pa$^{-1}$ at $T_g + 20$ °C. This observation supports the conclusion that T-DAP9 molecules have formed supramolecular polymers. The $J_e^0$ of T-DAP9 changes about 3 times from $T_g + 20$ °C to $T_g + 45$ °C. This trend also implies

the breakdown of the time–temperature superposition principle[43,50] and is consistent with the general behavior of polymers such as polystyrenes, as shown in Figure 6. It is important to recognize that the average chain length is expected to increase with decrease of temperature, as the hydrogen-bonding interactions get stronger. This effect could only lead to an increase of $J_e^0$. The observed decrease of $J_e^0$ of T-DAP9 with decrease of temperature is not directly related to the change of hydrogen-bonding strength but primarily due to the encroachment of segmental modes to chain modes near the glass transition temperature.[52]

Even without making any quantitative calculation, one could see from Figure 6 that the average chain length of T-DAP9 should be comparable to polystyrene of 3400 g/mol. The average chain length $\bar{N}$ of T-DAP9 can be further estimated using the following Rouse-like equation:[53]

$$\bar{N} = \bar{M}/M_0 \approx 2.5 J_e^0 \rho RT/M_0 \tag{4}$$

where $M_0$ is the molecular weight of T-DAP9 monomer, $R$ is the gas constant, and $\rho$ is the density of the melt, which is on the order of 1 g/cm$^3$. In the high temperature regime of 333 K with less interference of glass modes on the compliance, $\bar{N} \sim 7$, consistent with $\bar{N} \sim 8$ derived through association constant $K_a$ at the same temperature in eq 2.

**2. Nature of the Debye-like Relaxation.** The most intriguing feature in this type of supramolecular polymeric liquid is the discovery of the dielectric Debye-like relaxation process, which bears striking similarities to monoalcohols. In both cases, the spectra consist of a pronounced Debye-like relaxation accompanied by a weak stretched relaxation process on the high-frequency side. While recent studies have shown that the high-frequency relaxation, instead of the Debye-like process, is responsible for the structural ($\alpha$) relaxation of monoalcohols,[54] the exact nature of the Debye-like relaxation still remains an elusive subject of discussions.

For monoalcohols, the Debye-like relaxation exhibits a few interesting features. This mode is only observed in molecules with a single hydrogen-bonding center and absent in polyhydroxyl molecules except water.[55−57] Moreover, it has only revealed itself in dielectric experiments and is invisible in mechanical, calorimetric, and light scattering measurements.[54,58−60] Several possible origins of the Debye-like relaxation have been proposed, including rotation of the single hydroxyl dipole associated with breaking and re-forming hydrogen bond,[61] structural fluctuations,[62] micellar aggregates,[63,64] linear clusters,[65] and transient chain mode,[66,67] among others.

In living polymers, when the dissociation and recombination dynamics of hydrogen bonds are similar to or faster than the characteristic lifetime of an equivalent unbreakable chain mode, the chains relax at the same rate and lose the memory of their initial chain lengths, leading to nondispersion of terminal relaxation time, as predicted in the theoretical work on living polymer.[17,22] Although we cannot unambiguously identify a single-Maxwellian behavior in dynamic mechanical spectroscopy due to the contribution of the glassy modes in the high-frequency regime, a single-exponential relaxation behavior is revealed in dielectric measurement as the Debye mode. This Debye relaxation should thus correspond to the reorientation of the end-to-end dipole of the supramolecular chain, similar to type-A polymer with fast hydrogen-bond switching, which is closely coupled to the structural relaxation in the high

frequency range. The breaking of hydrogen bonds with increase of temperature leads to the decrease of the relaxation strength of Debye peak.

The relaxation time of the Debye-like and $\alpha$ process is further plotted as a function of reciprocal temperature in Figure 7. Both modes exhibit Vogel−Fulcher−Tammann (VFT)[68−70]
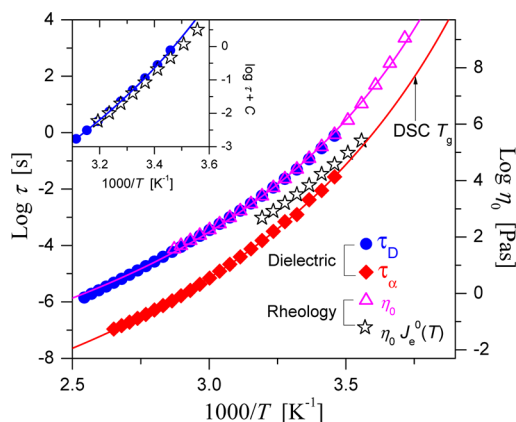


**Figure 7.** Temperature dependence of relaxation times and viscosity. Black open stars: relaxation time calculated by taking the product of viscosity and creep compliance. Here $J_e^0$ is determined directly from the viscoelastic spectra. Inset: comparison of the temperature dependence of the dielectric Debye-like relaxation time ($\tau_D$) and the mechanical terminal relaxation time ($\eta_0 J_e^0$). The mechanical relaxation time has been shifted by a constant $C$ to stress the difference between the two processes. Please note that the left and right $y$-axes cover the same orders of magnitude.

type temperature dependence. Extrapolating the $\alpha$ relaxation time to 100 s using the VFT equation yields a $T_g$ of 267 K, which agrees well with the result of differential scanning calorimetric measurement ($T_g$ = 266 K). This confirms the assignment of the high-frequency process to the structural ($\alpha$) relaxation of T-DAP9. In this regard, the behavior of T-DAP9 is analogous to that of monoalcohols, where the weak high-frequency process, instead of the pronounced Debye-like process, is responsible for the structural relaxation.

It is interesting to observe the very similar features in dielectric behaviors of T-DAP9 and monoalcohols. It is also important to recognize the significant difference between these two hydrogen-bonding liquids—while the Debye-like relaxation of monoalcohols has no mechanical signature, a separate chain relaxation mode is well-detected in the linear viscoelastic spectra of T-DAP9—and to draw an analogy between them regarding the formation of transient chain, as also elucidated on the potential of forming supramolecular polymer of T-DAP9 in the NMR and ESI-TWIM MS experiments. In order to gain a deeper insight about the Debye-like relaxation, the mechanical terminal relaxation time $\tau_0$ is added to Figure 7 as a comparison. Here, $\tau_0$ is calculated from the zero-shear viscosity $\eta_0$ and creep compliance $J_e^0$ as[43]

$$\tau_0 = \eta_0 J_e^0 \tag{5}$$

Since the creep compliance $J_e^0$ of T-DAP9 is not a constant near the glass transition, the temperature dependencies of $\tau_0$ and $\eta_0$ are different.

Comparison of the temperature dependence of $\tau_D$, $\tau_0$ ($\eta_0 J_e^0$), and $\eta_0$ in Figure 7 reveals that while the temperature dependence of $\tau_D$ and $\eta_0$ shows a perfect agreement, a weak

decoupling between $\tau_D$ and $\tau_0$ is discernible. This very weak decoupling could be ascribed to the transient nature of the supramolecular chain. When the dissociation and recombination occur fast, the dipole may not deviate away from the previous trajectory. The Debye mode, representing the normal mode of the fluctuating end-to-end dipole, could thus be possibly decoupled from the internal stress field. It is worth noting that although $\tau_0$, larger than $\tau_\alpha$, are ~1 decade apart from $\tau_D$, such a separation is not uncommon.[54]

While it is suggestive to assign the Debye-like relaxation to the chain relaxation of the associating polymer, other origins might not be absolutely excluded, considering the fact that the Debye-like relaxation of T-DAP9 appears to have the same temperature dependence as the zero-shear viscosity. For example, the fluctuation of a dipole in a dynamically fast homogeneous environment[71] was also proposed to produce Debye dispersion, and its relaxation rate is controlled by the viscosity of the surrounding medium.

## ■ CONCLUSION

In summary, using nuclear magnetic resonance, electrospray ionization mass spectrometry with traveling wave ion mobility separation, dielectric spectroscopy, and rheology, we show that the thymine and diamidopyridine-based molecule T-DAP9 forms supramolecular polymers through self-complementary triple hydrogen bonding. We demonstrate that the dielectric Debye-like relaxation is not unique to weakly hydrogen-bonded small molecular liquid such as monoalcohols but also exists in the supramolecular polymeric liquid driven by self-complementary hydrogen bonds. The high-frequency dielectric process is identified as the structural relaxation, whereas the low-frequency Debye-like relaxation is closely related to zero-shear viscosity. Unlike monoalcohols, where no corresponding mechanical relaxation can be found for the Debye-like process, the T-DAP9 supramolecular polymer does show a separate chain relaxation mode. The Debye mode is proposed to be associated with chain mode, although a weak decoupling between the mechanical terminal relaxation and dielectric Debye-like relaxation might be indicative of other viscosity-controlled mechanisms. We emphasize that T-DAP9 presents a novel class of materials with interesting relaxation and viscoelastic properties controlled significantly by the self-complementary hydrogen bonding.

## ■ ASSOCIATED CONTENT

**ⓢ Supporting Information**
Synthesis, characterization by using NMR, DSC, and creep experiments, and dielectric spectra analysis. This material is available free of charge via the Internet at http://pubs.acs.org.

## ■ AUTHOR INFORMATION

**Corresponding Author**
*E-mail: hmxiong@sjtu.edu.cn.
**Notes**
The authors declare no competing financial interest.

## ■ ACKNOWLEDGMENTS

## ■ REFERENCES

(1) Lehn, J.-M. *Supramolecular Chemistry: Concepts and Perspectives*; VCH: Weinheim, 1995.

(2) Lehn, J.-M. *Prog. Polym. Sci.* **2005**, *30*, 814−831.

(3) Ciferri, A. *Supramolecular Polymers*, 2nd ed.; CRC Press: Boca Raton, FL, 2005.

(4) Zimmerman, S. C.; Corbin, P. S. *Struct. Bonding (Berlin)* **2000**, *96*, 63−96.

(5) Wilson, A. J. *Soft Matter* **2007**, *3*, 409−25.

(6) Brunsveld, L.; Folmer, B. J. B.; Meijer, E. W.; Sijbesma, R. P. *Chem. Rev.* **2001**, *101*, 4071−4097.

(7) Cordier, P.; Tournilhac, F.; Soulie-Ziakovic, C.; Leibler, L. *Nature* **2008**, *451*, 977−980.

(8) Burnworth, M.; Tang, L. M.; Kumpfer, J. R.; Duncan, A. J.; Beyer, F. L.; Fiore, G. L.; Rowan, S. J.; Weder, C. *Nature* **2011**, *472*, 334−338.

(9) Thibault, R. J.; Hotchkiss, P. J.; Gray, M.; Rotello, V. M. *J. Am. Chem. Soc.* **2003**, *125*, 11249−11252.

(10) Niu, Z.; Huang, F.; Gibson, H. W. *J. Am. Chem. Soc.* **2011**, *133*, 2836−2839.

(11) Liu, Y. L.; Wang, Z. Q.; Zhang, X. *Chem. Soc. Rev.* **2012**, *41*, 5922−5932.

(12) Chen, G. S.; Jiang, M. *Chem. Soc. Rev.* **2011**, *40*, 2254−2266.

(13) Xue, M.; Yang, Y.; Chi, X.; Zhang, Z.; Huang, F. H. *Acc. Chem. Res.* **2012**, *45*, 1294−1308.

(14) Dimopoulos, A.; Wietor, J.-L.; Wübbenhorst, M.; Napolitano, S.; van Benthem, R. A. T. M.; de With, G.; Sijbesma, R. P. *Macromolecules* **2001**, *43*, 8664−8669.

(15) Wübbenhorst, M.; Folmer, B. J. B.; Van Turnhout, J.; Sijbesma, R. P.; Meijer, E. W. *IEEE. Trans. Trans. Dielectr. Electr. Insul.* **2001**, *8*, 365−371.

(16) Cates, M. E. *Macromolecules* **1987**, *20*, 2289−2296.

(17) Cates, M. E. *Europhys. Lett.* **1987**, *4*, 497−502.

(18) Cates, M. E.; Candau, S. J. *J. Phys.: Condens. Matter* **1990**, *2*, 6869−6892.

(19) Marques, C. M.; Turner, M. S.; Cates, M. E. *J. Chem. Phys.* **1993**, *99*, 7260−7266.

(20) Marques, C. M.; Turner, M. S.; Cates, M. E. *J. Non-Cryst. Solids* **1994**, *172−174*, 1168−1172.

(21) Milchev, A.; Rouault, Y.; Landau, D. P. *Phys. Rev. E* **1997**, *56*, 1946−1953.

(22) Stukalin, E. B.; Freed, K. F. *J. Chem. Phys.* **2006**, *125*, 184905.

(23) Green, M. S.; Tobolsky, A. V. *J. Chem. Phys.* **1946**, *14*, 80−92.

(24) Lodge, A. S. *Trans. Faraday. Soc.* **1956**, *52*, 120−130.

(25) Yamamoto, M. *J. Phys. Soc. Jpn.* **1956**, *11*, 413−421.

(26) Baxandall, L. G. *Macromolecules* **1989**, *22*, 1982−1988.

(27) Leibler, L.; Rubinstein, M.; Colby, R. H. *Macromolecules* **1991**, *24*, 4701−4707.

(28) Tanaka, F.; Edwards, S. F. *Macromolecules* **1992**, *25*, 1516−1523.

(29) Wang, S. Q. *Macromolecules* **1992**, *25*, 7003−7010.

(30) Rubinstein, M.; Semenov, A. N. *Macromolecules* **2001**, *34*, 1058−1068.

(31) Semenov, A. N.; Rubinstein, M. *Macromolecules* **2002**, *35*, 4821−4837.

(32) Lou, N.; Wang, Y. Y.; Li, H. X.; Sokolov, A. P.; Xiong, H. M. *Polymer* **2012**, *53*, 4455−4460.

(33) Sijbesma, R. P.; Beijer, F. H.; Brunsveld, L.; Folmer, B. J. B.; Ky Hirschberg, J. H. K.; Lange, R. F. M.; Lowe, J. K. L.; Meijer, E. W. *Science* **1997**, *278*, 1601−1604.

(34) Debye, P. *Verh. Dtsch. Phys. Ges.* **1913**, *15*, 777.

(35) Bowers, M. T.; Kemper, P. R.; von Helden, G.; van Koppen, P. A. M. *Science* **1993**, *260*, 1446−1451.

(36) Hoaglund-Hyzer, C. S.; Counterman, A. E.; Clemmer, D. E. *Chem. Rev.* **1999**, *99*, 3037−3079.

(37) Jiang, W.; Schafer, A.; Mohr, P. C.; Schalley, C. A. *J. Am. Chem. Soc.* **2010**, *132*, 2309−2320.

(38) Li, X.; Chan, Y.-T.; Newkome, G. R.; Wesdemiotis, C. *Anal. Chem.* **2011**, *83*, 6667−6674.

(39) Li, X.; Guo, L.; Casiano-Maldonado, M.; Zhang, D.; Wesdemiotis, C. *Macromolecules* **2011**, *44*, 4555−4564.

(40) Havriliak, S.; Negami, S. *Polymer* **1967**, *8*, 161−210.

(41) Ding, Y. F.; Sokolov, A. P. *Macromolecules* **2006**, *39*, 3322−3326.

(42) Sokolov, A. P.; Schweizer, K. S. *Phys. Rev. Lett.* **2009**, *102*, 248301.

(43) Ferry, J. D. *Viscoelastic Properties of Polymers*, 3rd ed.; Wiley: New York, 1980.

(44) The high-frequency spectra might be affected by the known issue of instrument compliance. However, all the quantitative analyses in study only deal with the terminal relaxation, which should be free from the compliance problem.

(45) Gray, R. W.; Harrison, G.; Lamb, J. *Proc. R. Soc. London, A* **1977**, *356*, 77−102.

(46) Ilhan, F.; Gray, M.; Rotello, V. M. *Macromolecules* **2001**, *34*, 2597−2601.

(47) Herbst, F.; Schröter, K.; Ilja, G.; Gröger, S.; Thurn-Albrecht, T.; Balbach, J.; Binder, W. H. *Macromolecules* **2010**, *43*, 10006−10016.

(48) Carothers, C. H. *Trans. Faraday Soc.* **1936**, *32*, 39−53.

(49) Allcock, H. R.; Lampe, F. W.; Mark, J. E. *Contemporary Polymer Chemistry*; Prentice Hall: Upper Saddle River, NJ, 2003.

(50) Plazek, D. J. *J. Rheol.* **1996**, *40*, 987−1014.

(51) Doi, M.; Edwards, S. F. *The Theory of Polymer Dynamics*; Oxford University Press: Oxford, 1986.

(52) Plazek, D. J.; Schlosser, E.; Schönhals, A.; Ngai, K. L. *J. Chem. Phys.* **1993**, *98*, 6488−6491.

(53) Rouse, P. E. *J. Chem. Phys.* **1953**, *21*, 1272.

(54) Jakobsen, B.; Maggi, C.; Christensen, T.; Dyre, J. C. *J. Chem. Phys.* **2008**, *129*, 184502.

(55) Döβ, A.; Paluch, M.; Sillescu, H.; Hinze, G. *Phys. Rev. Lett.* **2002**, *88*, 095701.

(56) Yomogida, Y.; Nozaki, R. In *Dielectric Relaxation Phenomena in Hydrogen-Bonded Liquids*, 5th International Workshop on Complex Systems, Sendai, Japan, 2008; Tokuyama, M., Oppenheim, I., Nishiyama, H., Eds.; American Institute of Physics: Sendai, Japan, 2008; pp 350−353.

(57) Nakanishi, M.; Nozaki, R. *Phys. Rev. E* **2011**, *83*, 051503.

(58) Hansen, C.; Stickel, F.; Berger, T.; Richert, R.; Fischer, E. W. *J. Chem. Phys.* **1997**, *107*, 1086−1093.

(59) Huth, H.; Wang, L.-M.; Schick, C.; Richert, R. *J. Chem. Phys.* **2007**, *126*, 104503.

(60) Wang, L.-M.; Tian, Y.; Liu, R.; Richert, R. *J. Chem. Phys.* **2008**, *128*, 084503.

(61) Hassion, F. X.; Cole, R. H. *J. Chem. Phys.* **1955**, *23*, 1756−1761.

(62) Johari, G. P.; Kalinovskaya, O. E.; Vij, J. K. *J. Chem. Phys.* **2001**, *114*, 4634−4642.

(63) Floridano, M. A.; Angell, C. A. *J. Chem. Phys.* **1989**, *91*, 2537−2543.

(64) MacCallum, J. L.; Tieleman, D. P. *J. Am. Chem. Soc.* **2002**, *124*, 15085−15093.

(65) Fragiadakis, D.; Roland, C. M.; Casalini, R. *J. Chem. Phys.* **2010**, *132*, 144505.

(66) Gainaru, C.; Meier, R.; Schildmann, S.; Lederle, C.; Hiller, W.; Rössler, E. A.; Böhmer, R. *Phys. Rev. Lett.* **2010**, *105*, 258303.

(67) Gainaru, C.; Kastner, S.; Mayr, F.; Lunkenheimer, P.; Schildmann, S.; Weber, H. J.; Hiller, W.; Loidl, A.; Böhmer, R. *Phys. Rev. Lett.* **2011**, *107*, 118304.

(68) Vogel, H. *J. Phys. Z.* **1921**, *22*, 645.

(69) Fulcher, G. S. *J. Am. Ceram. Soc.* **1925**, *8*, 339.

(70) Tammann, G.; Hesse, W. *Z. Anorg. Allg. Chem.* **1926**, *156*, 245.

(71) Anderson, J. E.; Ullman, R. *J. Chem. Phys.* **1967**, *47*, 2178−2184.

# SUPPORTING INFORMATION

## Dielectric Relaxation and Rheological Behavior of Supramolecular Polymeric Liquid

Nan Lou,[†] YangYang Wang,[‡] Xiaopeng Li,[§,⊥] Haixia Li,[†] Ping Wang,[∥] Chrys Wesdemiotis,[§] Alexei P. Sokolov,[‡] and Huiming Xiong[†*]

[†] Department of Polymer Science, Shanghai Jiao Tong University, Shanghai 200240
[‡] Chemical Sciences Division, Oak Ridge National Laboratory, Oak Ridge, TN 37831
[§] Department of Chemistry and Polymer Science, University of Akron, Akron, OH 44325
[⊥] Department of Chemistry and Biochemistry, Texas State University, San Marcos, TX 78666
[∥] Dow Chemicals Company Limited, Shanghai 201203
* Email: hmxiong@sjtu.edu.cn

**Experimental:**

**Materials.** 1,1,1,3,3,3-hexamethyldi-silazane (HMDS, 98%, Acros Organics) was purified by distillation under reduced pressure prior to use. Chlorotrimethylsilane (TMSCl, 98%, Acros Organics) was purified by distillation under nitrogen gas. Chelidamic acid (95+%, TCI), Decanoyl chloride (98+%, Sigma-Aldrich), 2,2-Dimethoxy-2-phenylacetophenone (DMPA, 99%, Acros Organics), Ammonia, ca. 7 N solution in methanol (Acros Organics), 8-Bromo-1-octene(97%, Sigma-Aldrich), 10% Pd-C (Sigma-Aldrich), thymine (99+%, Sigma-Aldrich), 1,6-Dibromohexane (97+%, Alfa Aesar) were all used as received. All other reagents were of analytical grade and used as received. All solvents were purified according to literature procedures.

**Synthesis:**
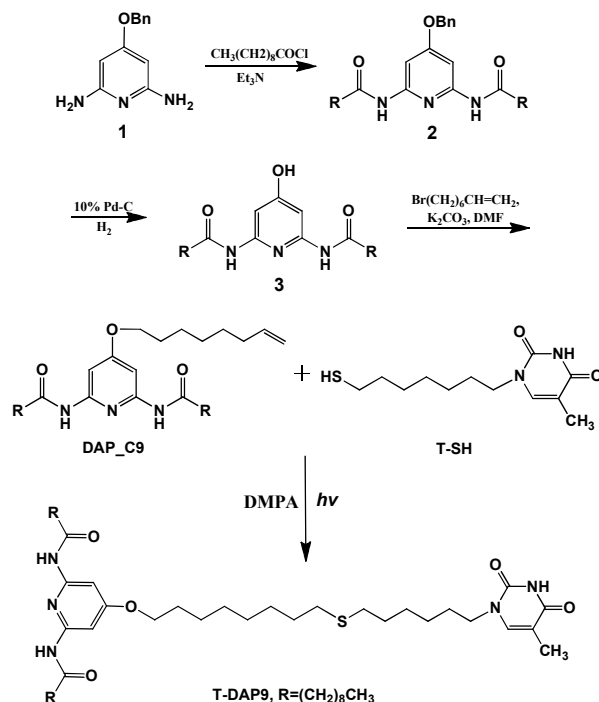


Scheme S1. Synthesis of T-DAP9.

**T-SH:** See Ref. S1.

**4-Oxybenzyl-2,6-Didecylamidopyridine (2):** A suspension of 4-Benzyloxy-2,6-pyridinediamine **1** (6.0 g, 27.9 mmol) and triethylamine (7.8 mL, 55.7 mmol) in dry $CH_2Cl_2$ (600 mL) was stirred at room temperature under nitrogen atmosphere. To this was added decanoyl chloride (11.8 mL, 55.7 mmol) in dry $CH_2Cl_2$ (300 mL) dropwise, and the mixture was stirred for 4h. The resulting solution was then extracted with water (3 × 200 mL). Concentration in vacuum, followed by chromatography (SiO2, Hex/EtOAc (1:1)) provided 12.7 g (87%) of the title compound as a cream-colored solid. $^1$H NMR(400MHz, $CDCl_3$, ppm) δ: 7.62 (s, 2H, CONH), 7.58 (s, 2H, $C_5H_2N$), 7.45-7.31 (m, 5H, $OCH_2ArH$), 5.13 (s, 2H, $OCH_2Ar$) 2.36 (t, 4H, $2COCH_2$), 1.70 (m, 4H, $2COCH_2CH_2$), 1.26 (s, 24H, $2(CH_2)_6$), 0.87 (t, 6H, $CH_3$).

**4-Hydroxyl-2,6-Didecylamidopyridine (3):** 4-Oxybenzyl-2,6-didecylamidopyridine **2** (4.0 g, 7.6 mmol) was stirred in the presence of 10% palladium on carbon (0.5 wt eq) in 60 mL of methanol for 6 h under hydrogen atmosphere. The suspension was filtered and the filtrate was evaporated to dryness in vacuum to obtain the title compound as white solid (3.0 g, 91%). $^1$H NMR (400MHz, DMSO-$d_6$, ppm) δ: 10.45 (s, 1H, ArOH), 9.71 (s, 2H, CONH), 7.24 (s, 2H, $C_5H_2N$), 2.32 (t, 4H, $2COCH_2$), 1.52 (m, 4H, $2COCH_2CH_2$), 1.24 (s, 24H, $2(CH_2)_6$), 0.83 (t, 6H, $CH_3$).

**4-Allyloctyl-2,6-Didecylamidopyridine (DAP9):** A solution of 4-Hydroxyl-2,6-Didecylamidopyridine **3** (2.5 g, 5.8 mmol), 8-bromo-1-octene (1.5 mL, 8.7 mmol), $K_2CO_3$ (0.82 g, 6.0 mmol) in 100mL DMF was stirred at 65 $^o$C for 24 h under nitrogen atmosphere. The solvent was removed under reduced pressure, then the solid was dissolved in $CH_2Cl_2$. After filtration, the liquid was concentrated in vacuo, followed by chromatography (SiO2, $CH_2Cl_2$/Hexane (3:1)) provided 3.0 g (96%) of the title compound as light yellow solid. $^1$H NMR (400MHz, $CDCl_3$, ppm) δ: 7.58 (s, 2H, CONH), 7.51(s, 2H, $C_5H_2N$), 5.85 - 5.76(m, 1H, $CH=CH_2$), 5.02-4.91(m, 2H, $CH=CH_2$), 4.02(t, 2H, $CH_2O$), 2.34(t, 4H, $2COCH_2$), 2.07-2.02(q, 2H, $CH-CH_2$), 1.77-1.65(m, 6H, $2COCH_2CH_2$, $OCH_2CH_2$), 1.48-1.32(m, 6H, $CH_2CH_2CH_2$), 1.26 (s, 24H, $2(CH_2)_6$), 0.87 (t, 6H, $CH_3$).

**2,6-Didecylamidopyridine-4-octyl-(N-1-mercapto-10-thymylhexane) (T-DAP9):** A solution of DAP9 (0.5 g, 0.92 mmol), T-SH (0.334 g, 1.38 mmol), and DMPA (12 mg, 0.046 mmol) were dissolved in 0.5 mL of THF, followed by irradiation (365 nm) for 1 h. The solvent was removed under reduced pressure, followed by chromatography (SiO2, Hex/EtOAc (2:1)) provided 0.36 g (83%) of the title compound as a high viscosity liquid.

**Characterization:**
**NMR concentration dependent experiments**
NMR concentration dependent experiments were carried at four different temperatures. At each temperature eight samples of different concentration were tested. The concentrations were 0.004 mol/L, 0.008 mol/L, 0.012 mol/L, 0.016 mol/L, 0.020 mol/L, 0.025 mol/L, 0.030 mol/L, 0.035 mol/L from dilute to concentrated, respectively. The experimental data for determination of the associate constant $K_a$ of T-DAP9 at different temperatures is shown below. $K_a$ is determined by using following equation (S2):

$$\delta - \delta_H = \frac{(\delta_C - \delta_H)}{2}\left\{\frac{[G]_t}{[H]_t} + 1 + \frac{1}{K_a[H]_t} - \sqrt{\left(\frac{[G]_t}{[H]_t} + 1 + \frac{1}{K_a[H]_t}\right)^2 - 4\frac{[G]_t}{[H]_t}}\right\}$$

Where, H, G, C represent the host, guest and the complex; $[H]_t$ and $[G]_t$ are the total concentration of host and guest molecule at initial state, respectively; $\delta_H$, $\delta_C$, $\delta$ are chemical shift of host and complex, and observed chemical shift. In our case, $[H]_t = [G]_t$.
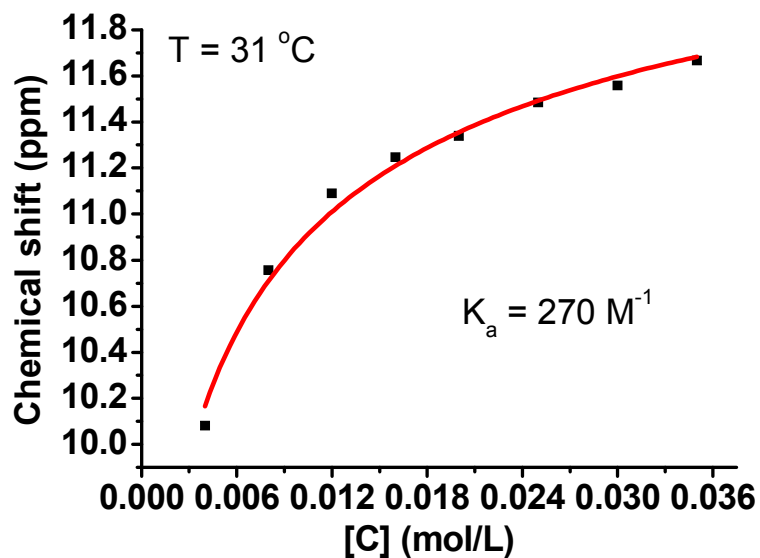


**Figure S1.** Determination of associate constant of T-DAP9 at temperature of 31 $^o$C.
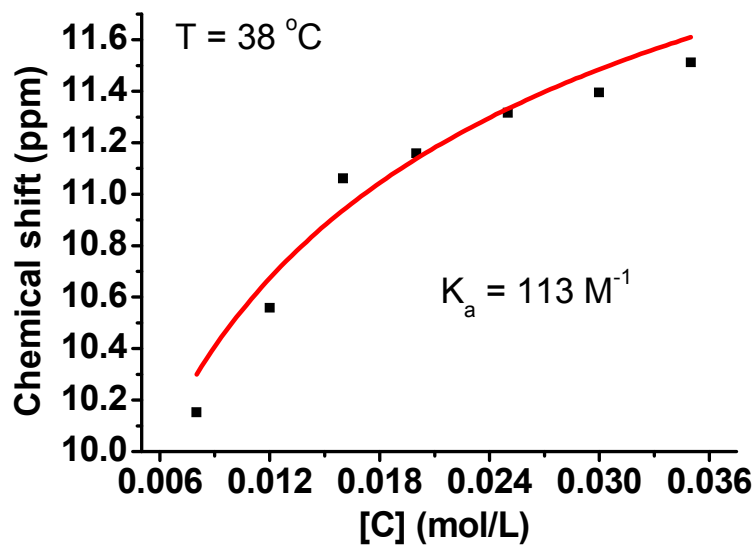


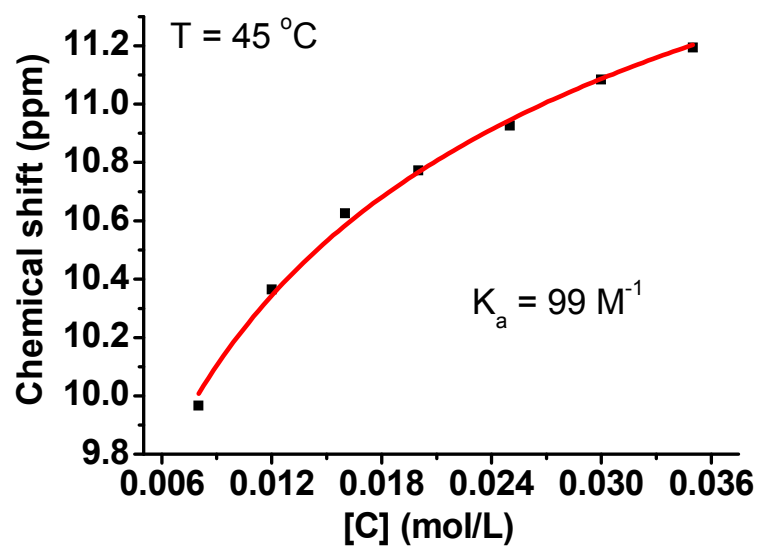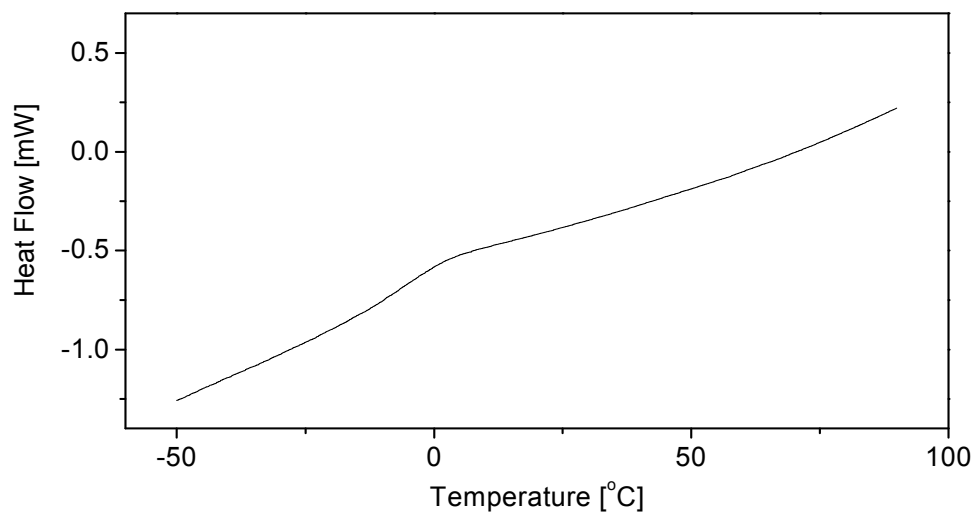**Figure S2.** Determination of associate constant of T-DAP9 at temperature of 38 $^o$C.

**Figure S3.** Determination of associate constant of T-DAP9 at temperature of 45 $^{\circ}$C.



**Figure S4**. DSC curve of T-DAP9 melt during cooling at 10 $^{\circ}$C/min.
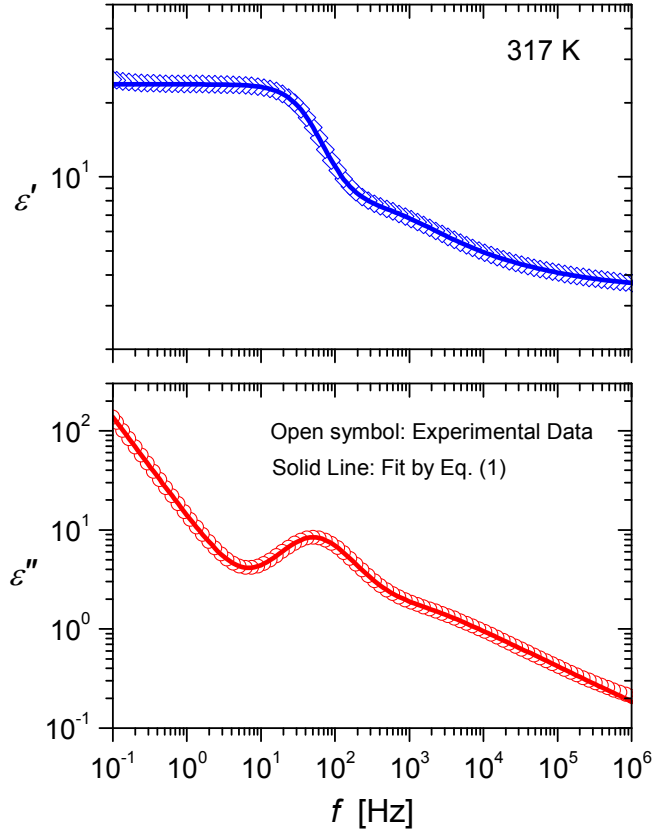
**Figure S5**. An example of the fit of the dielectric spectra with Eq. 1 (see the main text). Open symbols are experimental data and solids lines are the fits.
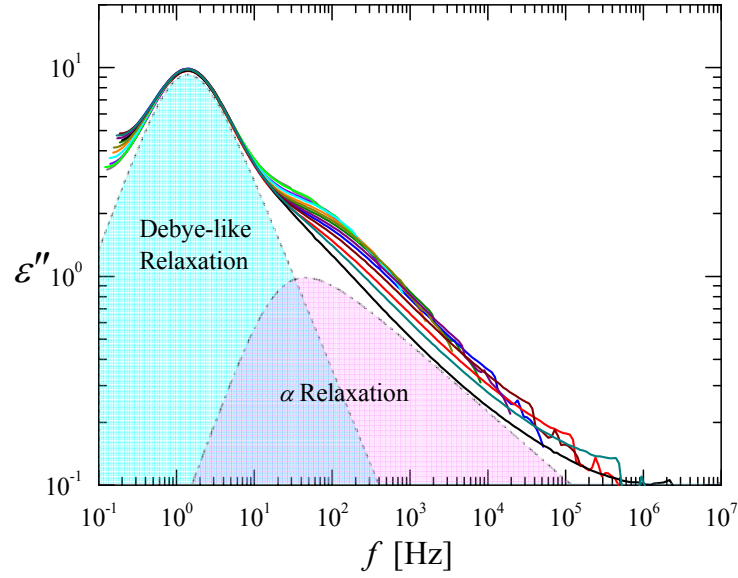


**Figure S6.** Shifted dielectric spectra at various temperatures with respect to the Debye mode at 297 K.
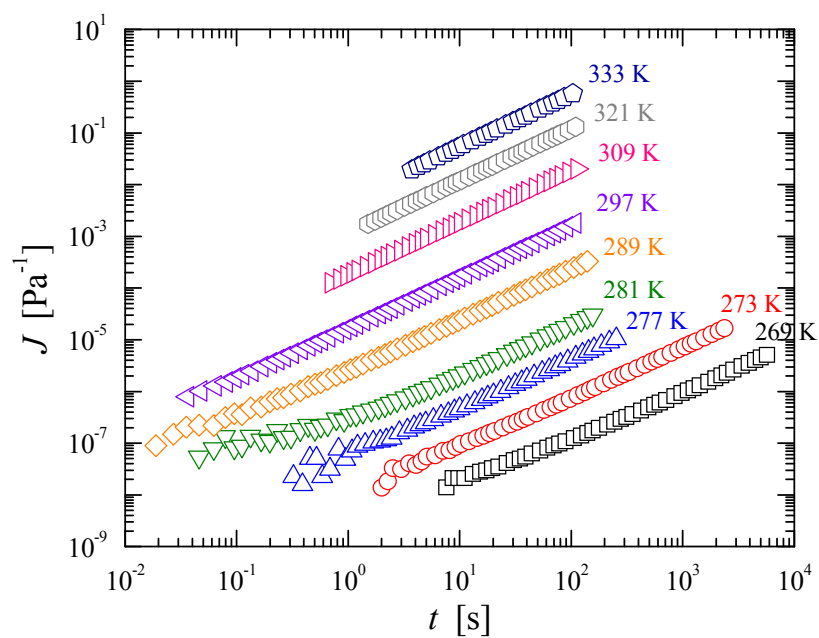
**Figure S7.** Creep compliance at various temperatures.

**Reference:**

(S1) Lou, N.; Wang, Y. Y.; Li, H. X.; Sokolov, A. P.; Xiong, H. M. *Polymer* **2012**, *53*, 4455.
(S2) Ilhan, F.; Gray, M.; Rotello, V. M. *Macromolecules* **2001**, *34*, 2597.